

Characterization of *in vitro* generated metabolites of the selective androgen receptor modulators S-22 and S-23 and *in vivo* comparison to post-administration canine urine specimens

Mario Thevis,^{a*} Enrico Gerace,^a Andreas Thomas,^a Simon Beuck,^a Hans Geyer,^a Nils Schlörer,^b Jeffrey D. Kearbey,^c James T. Dalton^c and Wilhelm Schänzer^a

Selective androgen receptor modulators (SARMs) have great therapeutic potential in various diseases including cancer cachexia, sarcopenia, and osteoporosis, and the number of drug candidates has been growing over the last decade. The SARM drug candidates S-22 and S-23 belong to one of the most advanced groups of androgen receptor modulators and are based on an arylpropionamide-derived core structure. Due to their anabolic effects, SARMs have been prohibited in elite sports and have been a subject of sports drug testing programmes since January 2008. Consequently, the structure of analytically useful urinary metabolites should be elucidated to provide targets for sensitive and retrospective analysis. In the present study, the phase-I and -II metabolism of S-22 and S-23 was simulated using hepatic human enzymes, and resulting metabolites were characterized by means of state-of-the-art mass spectrometric approaches employing high resolution/high accuracy Orbitrap mass spectrometry. Subsequently, the newly defined target compounds including the glucuronic acid conjugates of S-22 and S-23, their corresponding monohydroxylated and bishydroxylated analogs, as well as their B-ring depleted counterparts were implemented into an existing routine doping control procedure, which was examined for its specificity for the added substances. In order to obtain proof-of-concept data for authentic urine specimens, canine urine samples collected up to 72 h after oral administration of S-22 to dogs were analyzed using the established approach outlining the capability of the presented assay to detect the glucuronide of S-22 as well as the B-ring-depleted metabolite (M3) in all samples following therapeutic (31.4 µg/kg) dosing. Finally, M3 was chemically synthesized, characterized by nuclear magnetic resonance spectroscopy and high resolution/high accuracy mass spectrometry, and chosen as primary target for future doping control analyses. Copyright © 2010 John Wiley & Sons, Ltd.

Keywords: sport; mass spectrometry; S-22; Orbitrap; anabolics; metabolism

Introduction

Selective androgen receptor modulators (SARMs) have been the subject of determined medicinal research due to their potential beneficial properties for the treatment of various diseases. These include, for example, cancer cachexia, and sarcopenia, but also other indications such as age-related functional decline and geriatric frailty have been considered as potential areas of applications.^[1–5] Currently, dozens of drug candidates based on considerably different pharmacophores are in preclinical or clinical trials with arylpropionamide-derived SARMs representing the most advanced class of compounds.^[6] While the development of SARMs is an exciting medical advancement for individuals with disease-associated muscle wasting, osteoporosis, anemia, and different classifications of muscular dystrophies, concerns about an illicit use infiltrating the world of sport arose and were supported by recent findings of a non-approved drug candidate on the black market.^[7] Although no SARM product has been officially launched yet, such therapeutics may be particularly attractive to athletes as they presumably offer the desired anabolic effects

without typical undesirable effects commonly associated with anabolic androgenic steroid (mis)use. Consequently, since January 2008, the entire class of androgen receptor modulators has been prohibited in sports according to the anti-doping regulations of the World Anti-Doping Agency (WADA).^[8] Numerous detection methods for doping controls have been established during the last few years, and several approaches targeting the intact

* Correspondence to: Mario Thevis, Institute of Biochemistry - Center for Preventive Doping Research, German Sport University Cologne, Am Sportpark Müngersdorf 6, 50933 Cologne, Germany. E-mail: m.thevis@biochem.dshs-koeln.de

a Institute of Biochemistry - Center for Preventive Doping Research, German Sport University Cologne, Am Sportpark Müngersdorf 6, 50933 Cologne, Germany

b Institute of Organic Chemistry, University of Cologne, Greinstraße 4, 50939 Cologne, Germany

c GTx, Inc., 3 North Dunlap Street, Memphis, Tennessee 38163, USA

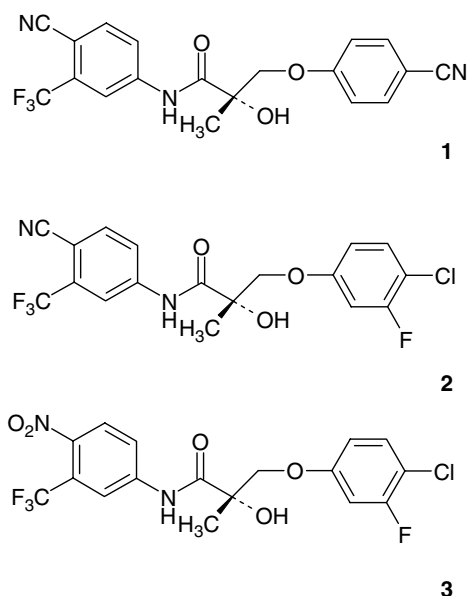


Figure 1. Chemical structures of **S-22** (1, mol wt = 389), **S-23** (2, mol wt_{monoisotopic} = 416), and **C-6** (3, mol wt_{monoisotopic} = 436).

compounds as well as *in vitro* or chemically derived metabolites were reported.^[9–14]

In the present study, the *in vitro* metabolism of the SARM drug candidates **S-22** and **S-23** (Figure 1, **1** and **2**, respectively) was studied using high resolution/high accuracy mass spectrometry. **S-22** [3-(4-cyano-phenoxy)-N-(4-cyano-3-trifluoromethylphenyl)-2-hydroxy-2-methyl-propionamide] has demonstrated higher *in vivo* anabolic activity than other advanced candidates such as **S-4**, attributed to the cyano substituent in the *para*-position of the B-ring that proved structurally, pharmacologically and metabolically favorable.^[15–17] The *in vivo* half-life of **S-22** in rats was approximately 6 h,^[16] and recent studies outlined mechanisms of action that are different compared to those resulting from steroidal agents such as dihydrotestosterone.^[18] **S-23** [3-(3-fluoro-4-chlorophenoxy)-N-(4-cyano-3-trifluoromethylphenyl)-2-hydroxy-2-methyl-propionamide] has primarily been investigated for its utility as a hormonal male contraceptive, being a structural analog to **C-6** (Figure 1, **3**).^[19] An increase in lean body mass associated with a reduction of fat in a dose-dependent manner was also reported.^[20] As a consequence, potential metabolites of both SARMS (**S-22** and **S-23**) were generated using *in vitro* metabolism models as a first step towards determining those metabolites which should be targeted in sports drug testing of urine samples. The derived compounds were characterized and implemented into an existing initial testing procedure. Subsequently, canine urine samples obtained from oral administration studies were analyzed for the predicted analytes to provide a first proof-of-principle. This approach did not allow a direct intra-species *in vivo/in vitro* correlation of the results but served the purpose of testing the established assay. One of the most prominent metabolites (**M3**, Figure 2) was chemically synthesized, characterized using nuclear magnetic resonance spectroscopy (NMR) and mass spectrometry to be employed as reference material for future doping control analyses.

Experimental

Reference compounds, chemicals and reagents

Reference materials of **S-22** and **S-23** were provided by GTx Inc. (Memphis, TN, USA). Reduced nicotinamide adenine dinucleotide phosphate tetrasodium salt (NADPH) was obtained from Roche Diagnostic (Mannheim, Germany), adenosine 3'-phosphate 5'-phosphosulphate (PAPS) was from Calbiochem (La Jolla, CA, USA), *D*-saccharic acid 1,4-lactone and uridine 5'-diphosphoglucuronic acid (UDPGA) were from Sigma (St Louis, MA), and human liver microsomal (HLM) and S-9 fraction were purchased from BD Gentest (Woburn, MA, USA) and represented pools of several individual donors (mixed gender). All solvents used were of analytical grade and deionized water was supplied by a MilliQ apparatus.

In vitro metabolism

Metabolic incubations were performed in Eppendorf reaction tubes in a total volume of 100 μ L. The reaction mixtures contained 10 μ M of **S-22** or **S-23** (10 μ L of a 100 μ M solution in dimethyl sulfoxide, DMSO) and 5 mM of NADPH in 50 mM potassium phosphate buffer (pH 7.4) containing 5 mM MgCl₂. Two blank samples were analyzed with each incubation batch. One blank specimen lacked the substrate (i.e. **S-22** or **S-23**) and the other one lacked the enzymatic protein to test for potential interferences caused by contamination of the substrate or non-enzymatic reactions during incubation. *D*-saccharic acid-1,4-lactone (5 mM) was added as glucuronidase inhibitor in those samples further undergoing glucuronidation as the phase-II metabolism. The samples were mixed gently prior to the addition of the S-9 fraction protein (20 μ g/incubation), and specimens were incubated at 37 °C for 2 h with continuous agitation. The subsequent phase-II metabolism reactions were initiated by the addition of UDPGA (5 mM) or PAPS (20 μ M) for glucuronidation or sulfonation, respectively. The reaction mixture was incubated for an additional period of 2 h at 37 °C with continuous mixing. Incubations were terminated by adding 100 μ L of ice-cold acetonitrile to precipitate the protein and specimens were centrifuged at 10000 $\times g$ for 5 min before the supernatant was transferred to a fresh Eppendorf test tube.

Sample purification

In order to purify the generated target analytes, liquid-liquid extraction (LLE) under acidic conditions (pH 4.5–5.0) was conducted. Prior to LLE, the acetonitrile content was evaporated using a vacuum centrifuge, and 20 μ L of acetic acid (2%) was added to the aqueous residue. The specimens were then extracted twice with 500 μ L of ethyl acetate, the organic layers were combined, evaporated to dryness, and the dry residues were reconstituted in 50 μ L of the mobile phase before injection into the LC-MS/MS system.

Liquid chromatography-tandem mass spectrometry (LC-MS/MS)

In agreement with an earlier study,^[21] all samples were analyzed using a LC-MS/MS system consisting of an API 4000 QTrap mass spectrometer (Darmstadt, Germany) coupled to an Agilent 1100 Series HPLC system (Walldbronn, Germany). Chromatographic separation was accomplished on a XTerra RP₁₈ Isis column (3.5 μ m, 2.1 \times 150 mm; Waters, Milford, MA, USA). The flow rate was set to

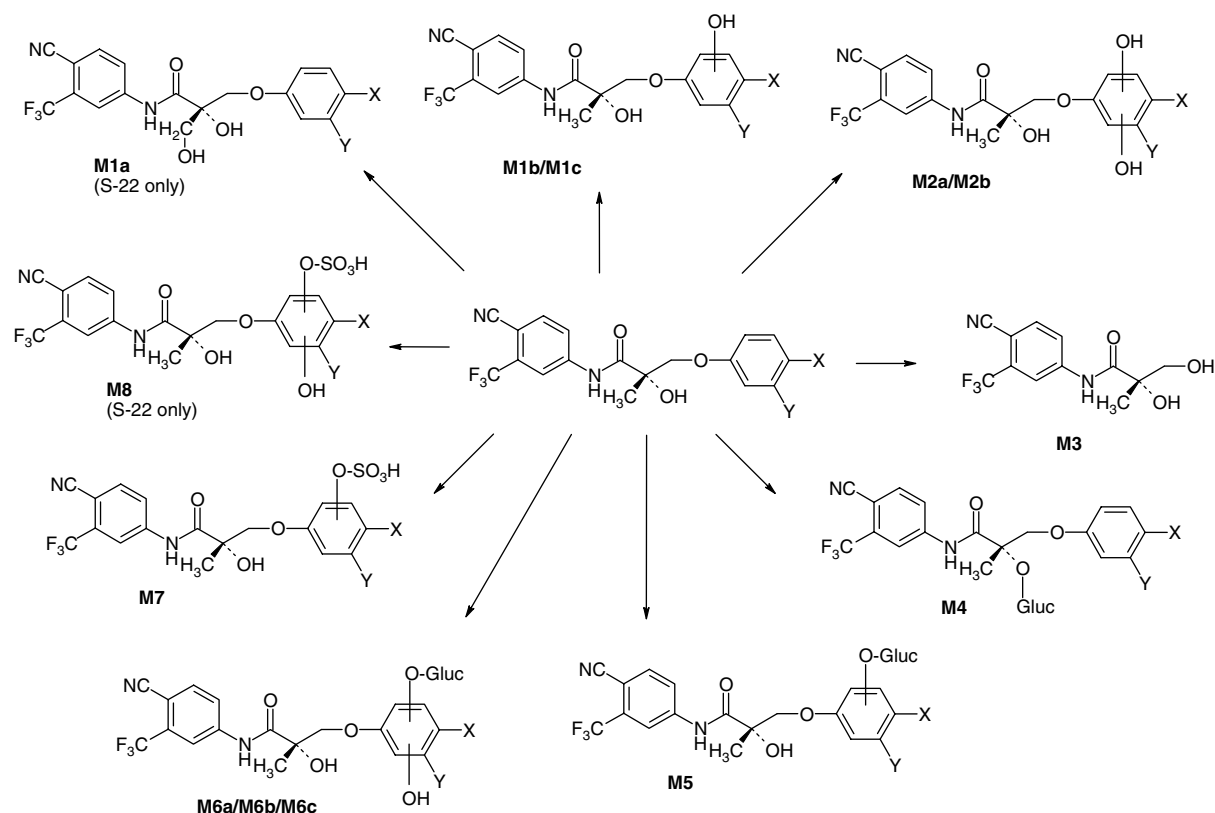


Figure 2. Summary of metabolites of **S-22** (X = CN, Y = H) and **S-23** (X = Cl, Y = F) identified in *in vitro* metabolism experiments.

250 $\mu\text{L}/\text{min}$ and the mobile phase consisted of 5 mM ammonium acetate with 0.1% acetic acid (solvent A) and methanol (solvent B). Gradient elution was employed after an initial isocratic step at 20% B (3 min), linearly increasing to 100% B in 9 min. All mass spectrometry (MS) measurements were conducted using negative electrospray ionization (ESI) at an ion source temperature of 500 $^{\circ}\text{C}$ and an ionspray voltage of -4200 V . The MS experiments included full-scan (m/z 100–700), product ion scan (MS^2 and MS^3), and multiple reaction monitoring (MRM) analyses, with the latter approach being of interest for routine doping control assays (Tables 1 and 2). Nitrogen was obtained from a CMC generator (CMC, Eschbach, Germany) and used as collision gas at $5 \times 10^{-3}\text{ Pa}$.

Further to the above reported low-resolution mass spectrometric approach, high resolution/high accuracy mass spectrometry data were recorded to determine the elemental composition of the metabolites of S-22 and S-23. These analyses were conducted on a Thermo Exactive mass spectrometer (operated at a resolving power of 25 000, full-width half maximum) interfaced to a Thermo Accela LC system (Thermo, Bremen, Germany). The LC conditions were identical to those used with the low resolution set-up. The Exactive mass spectrometer was operated in negative ESI mode and calibrated using the manufacturer's calibration mixture allowing for mass accuracies $<5\text{ ppm}$. The ionization voltage was -3500 V and the capillary temperature set to 275 $^{\circ}\text{C}$. The gas supplied to the curved linear ion trap (CLT) was nitrogen also obtained from a CMC generator (*vide supra*).

Dog urine specimens

In order to test for the presence of the *in vitro* derived metabolites of S-22 in authentic urine samples, specimens collected from animal

studies were utilized. Since dog *in vitro* and *in vivo* studies were conducted with other arylpropionamide-derived SARMs earlier and highly comparable results were obtained in an interspecies-comparison of human and dog S-9 fraction incubations,^[22,23] the dog model was considered suitable also for the present investigations. The administration studies were conducted under the auspices of animal protocol reviewed and approved by the Institutional Laboratory Animal Care and Use Committee at the University of Tennessee Health Science Center. Two female beagle dogs were purchased from Marshall Farms (North Rose, NY, USA). One dog (weighing 8.8 kg) received an oral dose (0.0314 mg/kg) of S-22 in a volume of 5 mL, while the other dog (weighing 10.4 kg) received an oral dose (30 mg/kg) in a volume of 10 mL. The dosing solution was prepared by dissolving S-22 into the appropriate volume of polyethylene glycol 300. Urine samples were collected over four periods: pre-dose, 0–24 hrs, 24–48 hrs, and 48–72 hrs.

Urine sample preparation

In order to recover phase-I and -II metabolites from the urine samples, 2 mL aliquots were prepared according to an established doping control procedure.^[9] In brief, the method consisted of a conventional solid-phase extraction (SPE) using PAD-1 adsorber resin. The retained analytes were washed with water and eluted with methanol, the eluate was concentrated to dryness and re-constituted in 200 μL of methanol/0.1% formic acid (1 : 1, v : v) to be subjected to LC-MS/MS.

Test for specificity and ion suppression/enhancement effects

Following the enzymatic synthesis and characterization of *in vitro* derived metabolites of S-22 and S-23, the specificity of a routine

Table 1. Elemental compositions of deprotonated molecules $[M - H]^-$ of **S-22** and **M1-M8** with resulting diagnostic product ions using high resolution/high accuracy MS/MS experiments. Product ions of routine doping control analyses are expressed in bold

Cmp.	metabolic reaction(s)	$[M - H]^-$ (<i>m/z</i>)	elemental comp. (exp.)	error (ppm)	CE*	Product ion (<i>m/z</i>)	elemental comp. (exp.)	error (ppm)	cleaved species	found in canine urine
S-22		388.0910	$C_{19}H_{13}O_3N_3F_3$	-1.0	30	269.0536	$C_{12}H_8O_2N_2F_3$	-2.8	C_7H_5NO	yes
						241.0586	$C_{11}H_8ON_2F_3$	-3.4	C_7H_5NO, CO	
						185.0323	$C_8H_4N_2F_3$	-5.0	$C_{11}H_9NO_3$	
						118.0294	C_7H_4ON	-4.0	$C_{12}H_9O_2N_2F_3$	
M1a	hydroxylation	404.0866	$C_{19}H_{13}O_4N_3F_3$	0.5	30	285.0494	$C_{12}H_8O_3N_2F_3$	0.7	C_7H_5NO	yes
						255.0393	$C_{11}H_6O_2N_2F_3$	0.7	C_7H_5NO, CH_2O	
						185.0329	$C_8H_4N_2F_3$	-1.5	$C_{11}H_9NO_4$	
						118.0294	C_7H_4ON	-4.0	$C_{12}H_9O_3N_2F_3$	
M1b	hydroxylation	404.0867	$C_{19}H_{13}O_4N_3F_3$	0.9	30	269.0541	$C_{12}H_8O_2N_2F_3$	-0.8	$C_7H_5NO_2$	yes
						185.0330	$C_8H_4N_2F_3$	-1.2	$C_{11}H_9NO_4$	
						134.0244	$C_7H_4O_2N$	-2.9	$C_{12}H_9O_2N_2F_3$	
						269.0540	$C_{12}H_8O_2N_2F_3$	-1.2	$C_7H_5NO_2$	
M1c	hydroxylation	404.0866	$C_{19}H_{13}O_4N_3F_3$	0.5	30	185.0329	$C_8H_4N_2F_3$	-1.5	$C_{11}H_9NO_4$	
						134.0243	$C_7H_4O_2N$	-3.4	$C_{12}H_9O_2N_2F_3$	
						269.0544	$C_{12}H_8O_2N_2F_3$	0.1	$C_7H_5NO_3$	
						150.0193	$C_7H_4O_3N$	-2.4	$C_{12}H_9O_2N_2F_3$	
M2a	bishydroxylation	420.0815	$C_{19}H_{13}O_5N_3F_3$	0.6	30	269.0535	$C_{12}H_8O_2N_2F_3$	-3.2	$C_7H_5NO_3$	yes
						150.0193	$C_7H_4O_3N$	-2.4	$C_{12}H_9O_2N_2F_3$	
						257.0543	$C_{11}H_8O_2N_2F_3$	-0.2	CH_2O	
						214.0483	$C_{10}H_7ONF_3$	-0.8	$C_2H_3O_2N$	
M2b	bishydroxylation	420.0815	$C_{19}H_{13}O_5N_3F_3$	0.6	30	213.0279	$C_9H_4ON_2F_3$	-0.8	$C_3H_6O_2$	
						185.0328	$C_8H_4N_2F_3$	-2.1	$C_4H_6O_3$	
						445.0864	$C_{18}H_{16}O_8N_2F_3$	-0.1	C_7H_5ON	
						388.0915	$C_{19}H_{13}O_3N_3F_3$	0.3	$C_6H_8O_6$	
M3	O-dephenylation	287.0649	$C_{12}H_{10}O_3N_2F_3$	-0.2	30	287.0649	$C_{12}H_{10}O_3N_2F_3$	-0.2	$C_{13}H_{11}O_6N$	yes
						269.0544	$C_{12}H_8O_2N_2F_3$	0.3	$C_6H_8O_6, C_7H_5NO$	
						185.0329	$C_8H_4N_2F_3$	-1.5	$C_6H_8O_6, C_{11}H_9NO_3$	
						118.0294	C_7H_4ON	-4.0	$C_6H_8O_6, C_{12}H_9O_2N_2F_3$	
M4	glucuronidation	564.1232	$C_{25}H_{21}O_9N_3F_3$	-0.6	30	404.0864	$C_{19}H_{13}O_4N_3F_3$	0.0	$C_6H_8O_6$	yes
						310.0568	$C_{13}H_{12}O_8N$	-0.2	$C_{12}H_9O_2N_2F_3$	
						269.0544	$C_{12}H_8O_2N_2F_3$	0.3	$C_6H_8O_6, C_7H_5NO_2$	
						134.0243	$C_7H_4O_2N$	-3.5	$C_6H_8O_6, C_{12}H_9O_2N_2F_3$	
M5	hydroxylation, glucuronidation	580.1184	$C_{25}H_{21}O_{10}N_3F_3$	-0.1	30	420.0813	$C_{19}H_{13}O_5N_3F_3$	0.0	$C_6H_8O_6$	no
						326.0517	$C_{13}H_{12}O_9N$	-0.3	$C_{12}H_9O_2N_2F_3$	
						150.0193	$C_7H_4O_3N$	-2.4	$C_6H_8O_6, C_{12}H_9O_2N_2F_3$	
						420.0815	$C_{19}H_{13}O_5N_3F_3$	0.5	$C_6H_8O_6$	
M6a	bishydroxylation, glucuronidation	596.1135	$C_{25}H_{21}O_{11}N_3F_3$	0.2	30	326.0516	$C_{13}H_{12}O_9N$	-0.5	$C_{12}H_9O_2N_2F_3$	no
						150.0193	$C_7H_4O_3N$	-2.4	$C_6H_8O_6, C_{12}H_9O_2N_2F_3$	
						420.0815	$C_{19}H_{13}O_5N_3F_3$	0.5	$C_6H_8O_6$	
						326.0518	$C_{13}H_{12}O_9N$	0.1	$C_{12}H_9O_2N_2F_3$	
M6b	bishydroxylation, glucuronidation	596.1135	$C_{25}H_{21}O_{11}N_3F_3$	0.2	30	150.0193	$C_7H_4O_3N$	-2.4	$C_6H_8O_6, C_{12}H_9O_2N_2F_3$	no
						420.0815	$C_{19}H_{13}O_5N_3F_3$	0.5	$C_6H_8O_6$	
						326.0518	$C_{13}H_{12}O_9N$	0.1	$C_{12}H_9O_2N_2F_3$	
						150.0193	$C_7H_4O_3N$	-2.4	$C_6H_8O_6, C_{12}H_9O_2N_2F_3$	
M6c	bishydroxylation, glucuronidation	596.1135	$C_{25}H_{21}O_{11}N_3F_3$	0.2	30	420.0815	$C_{19}H_{13}O_5N_3F_3$	0.5	$C_6H_8O_6$	no
						326.0518	$C_{13}H_{12}O_9N$	0.1	$C_{12}H_9O_2N_2F_3$	
						150.0193	$C_7H_4O_3N$	-2.4	$C_6H_8O_6, C_{12}H_9O_2N_2F_3$	
						420.0815	$C_{19}H_{13}O_5N_3F_3$	0.5	$C_6H_8O_6$	
M7	hydroxylation, sulfonation	484.0430	$C_{19}H_{13}O_7N_3F_3S$	-0.3	30	404.0863	$C_{19}H_{13}O_4N_3F_3$	-0.1	SO_3	yes
						269.0538	$C_{12}H_8O_2N_2F_3$	-2.1	$SO_3, C_7H_5NO_2$	
						134.0243	$C_7H_4O_2N$	-3.5	$SO_3, C_{12}H_9O_2N_2F_3$	
						420.0813	$C_{19}H_{13}O_5N_3F_3$	0.0	SO_3	
M8	bishydroxylation, sulfonation	500.0382	$C_{19}H_{13}O_8N_3F_3S$	0.3	30	150.0194	$C_7H_4O_3N$	-2.1	$SO_3, C_{12}H_9O_2N_2F_3$	no

* CE = collision energy (eV)

Table 2. Elemental compositions of deprotonated molecules $[M - H]^-$ of **S-23** and **M1-M7** with resulting diagnostic product ions using high resolution/high accuracy MS/MS experiments. Product ions of routine doping control analyses are expressed in bold

Cmp.	metabolic reaction(s)	$[M - H]^-$ (<i>m/z</i>)	elemental comp. (exp.)	error (ppm)	CE*	Product ion (<i>m/z</i>)	elemental comp. (exp.)	error (ppm)	cleaved species
S-23		415.0480	$C_{18}H_{12}O_3N_2ClF_4$	0.4	30	269.0543	$C_{12}H_8O_2N_2F_3$	0.1	C_6H_4OCIF
						241.0593	$C_{11}H_8ON_2F_3$	−0.5	C_6H_4OCIF , CO
						185.0328	$C_8H_4N_2F_3$	−2.1	$C_{10}H_8O_3ClF$
						144.9858	C_6H_3OCIF	−3.0	$C_{12}H_9O_2N_2F_3$
M1b	hydroxylation	431.0427	$C_{18}H_{12}O_4N_2ClF_4$	−0.1	30	269.0543	$C_{12}H_8O_2N_2F_3$	0.1	$C_6H_4O_2ClF$
						185.0328	$C_8H_4N_2F_3$	−2.1	$C_{10}H_8O_4ClF$
						160.9807	$C_6H_3O_2ClF$	−1.3	$C_{12}H_9O_3N_2F_3$
M1c	hydroxylation	431.0428	$C_{18}H_{12}O_4N_2ClF_4$	0.3	30	269.0544	$C_{12}H_8O_2N_2F_3$	0.2	$C_6H_4O_2ClF$
						185.0329	$C_8H_4N_2F_3$	−1.8	$C_{10}H_8O_4ClF$
						160.9808	$C_6H_3O_2ClF$	−2.0	$C_{12}H_9O_3N_2F_3$
M2	bishydroxylation	447.0376	$C_{18}H_{12}O_5N_2ClF_4$	0.0	30	269.0544	$C_{12}H_8O_2N_2F_3$	0.1	$C_6H_4O_3ClF$
						176.9757	$C_6H_3O_3ClF$	−2.1	$C_{12}H_9O_2N_2F_3$
M3	O-dephenylation	287.0649	$C_{12}H_{10}O_3N_2F_3$	−0.2	30	257.0543	$C_{11}H_8O_2N_2F_3$	−0.2	CH ₂ O
						185.0329	$C_8H_4N_2F_3$	−1.9	C ₄ H ₆ O ₃
M4	glucuronidation	591.0799	$C_{24}H_{20}O_9N_2ClF_4$	−0.1	30	445.0864	$C_{18}H_{16}O_8N_2F_3$	−0.1	C_6H_4OCIF
						415.0474	$C_{18}H_{12}O_3N_2ClF_4$	−0.9	C ₆ H ₈ O ₆
						287.0649	$C_{12}H_{10}O_3N_2F_3$	−0.2	$C_{12}H_{10}O_6ClF$
						269.0544	$C_{12}H_8O_2N_2F_3$	0.3	C ₆ H ₈ O ₆ , C_6H_4OCIF
						185.0330	$C_8H_4N_2F_3$	−1.2	C ₆ H ₈ O ₆ , $C_{10}H_8O_3ClF$
						144.9858	C_6H_3OCIF	−2.4	C ₆ H ₈ O ₆ , $C_{12}H_9O_2N_2F_3$
M5	hydroxylation, glucuronidation	607.0748	$C_{24}H_{20}O_{10}N_2ClF_4$	−0.1	30	431.0426	$C_{18}H_{12}O_4N_2ClF_4$	−0.2	C ₆ H ₈ O ₆
						337.0132	$C_{12}H_{11}O_8ClF$	−0.1	$C_{12}H_9O_2N_2F_3$
						269.0544	$C_{12}H_8O_2N_2F_3$	0.3	C ₆ H ₈ O ₆ , $C_6H_4O_2ClF$
						160.9807	$C_6H_3O_2ClF$	−2.0	C ₆ H ₈ O ₆ , $C_{12}H_9O_2N_2F_3$
M6a	bishydroxylation, glucuronidation	623.0698	$C_{24}H_{20}O_{11}N_2ClF_4$	0.2	30	447.0378	$C_{18}H_{12}O_5N_2ClF_4$	0.4	C ₆ H ₈ O ₆
						176.9762	$C_6H_3O_3ClF$	0.9	C ₆ H ₈ O ₆ , $C_{12}H_9O_2N_2F_3$
M6b	bishydroxylation, glucuronidation	623.0698	$C_{24}H_{20}O_{11}N_2ClF_4$	0.2	30	447.0378	$C_{18}H_{12}O_5N_2ClF_4$	0.4	C ₆ H ₈ O ₆
						176.9758	$C_6H_3O_3ClF$	−1.1	C ₆ H ₈ O ₆ , $C_{12}H_9O_2N_2F_3$
M6c	bishydroxylation, glucuronidation	623.0698	$C_{24}H_{20}O_{11}N_2ClF_4$	0.2	30	447.0380	$C_{18}H_{12}O_5N_2ClF_4$	0.7	C ₆ H ₈ O ₆
						176.9758	$C_6H_3O_3ClF$	−1.1	C ₆ H ₈ O ₆ , $C_{12}H_9O_2N_2F_3$
M7a	hydroxylation, sulfonation	510.9995	$C_{18}H_{12}O_7N_2ClF_4S$	0.0	30	431.0426	$C_{18}H_{12}O_4N_2ClF_4$	−0.2	SO ₃
						269.0544	$C_{12}H_8O_2N_2F_3$	0.3	SO ₃ , $C_6H_4O_2ClF$
						160.9813	$C_6H_3O_2ClF$	1.2	SO ₃ , $C_{12}H_9O_2N_2F_3$
M7b	hydroxylation, sulfonation	510.9994	$C_{18}H_{12}O_7N_2ClF_4S$	−0.2	30	431.0429	$C_{18}H_{12}O_4N_2ClF_4$	0.4	SO ₃
						269.0544	$C_{12}H_8O_2N_2F_3$	0.3	SO ₃ , $C_6H_4O_2ClF$
						160.9807	$C_6H_3O_2ClF$	−2.3	SO ₃ , $C_{12}H_9O_2N_2F_3$

* CE = collision energy (eV)

doping control procedure concerning the identified analytes was determined. Therefore, extracted metabolite mixtures were analyzed to determine respective retention times in LC-MS/MS measurements and 10 different human urine samples obtained from healthy male (5) and female (5) donors were analyzed to study the biological background at expected retention times. In order to estimate ion suppression effects possibly caused by matrix interference, four different blank urine samples and solvent only were analyzed with continuous co-infusion of S-22 and S-23 (solution concentration 0.5 pg/μL, flow rate 5 μL/min) via T-connector according to literature recommendations.^[24,25]

Synthesis and characterization of target metabolite M3

Full structural characterization of a potential target compound referred to as **M3** (Figure 2) was accomplished by chemical synthesis of respective reference material and subsequent NMR

and LC-ESI-high resolution/high accuracy mass spectrometry measurements.

During the process of synthesizing **S-22** and **S-23**,^[26–28] the aryl-propionamide core structure is prepared using the intermediate reaction product 3-bromo-N-(4-cyano-3-trifluoromethyl-phenyl)-2-hydroxy-2-methyl-propionamide. In the course of conversion into the respective epoxide, **M3** (N-(4-cyano-3-trifluoromethyl-phenyl)-2,3-dihydroxy-2-methyl-propionamide) is obtained as by-product and was purified by reversed-phase column chromatography (PAD-I, water/methanol 60:40, v:v) followed by silica gel flash chromatography (*tert*-butyl methyl ether/methanol 10:1, v:v). One mg of the final product was dissolved in CDCl₃ and characterized by ¹H and ¹³C nuclear magnetic resonance spectroscopy (NMR) with ¹H (600 MHz), H,H-COSY, H,C-HMQC, and H,C-HMBC experiments employing a Bruker AV 600 instrument (Bruker, Karlsruhe, Germany) equipped with a 5 mm inverse probe head (z-gradient coil). The elemental composition of the refer-

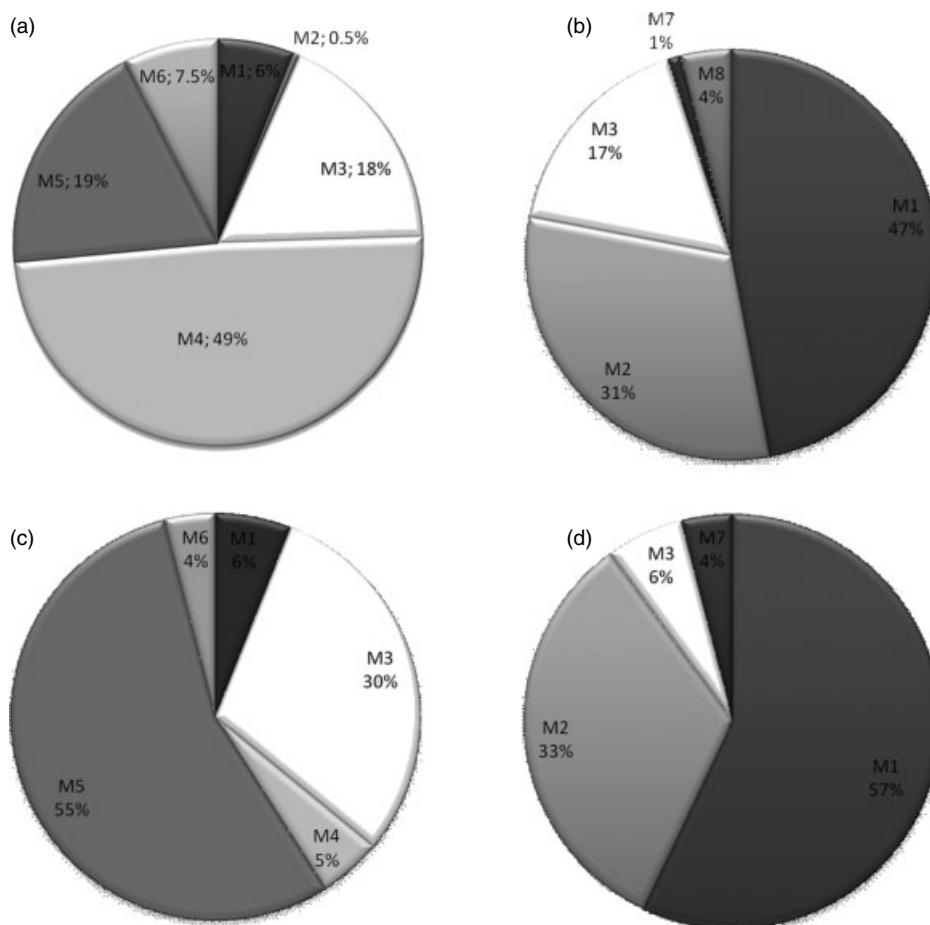


Figure 3. Metabolites found in *in vitro* experiments of S-22 and S-23 using phase-I and phase-II reaction conditions: (A) S-22, phase-I metabolism followed by glucuronidation; (B) S-22, phase-I metabolism followed by sulfonation; (C) S-23, phase-I metabolism followed by glucuronidation; (D) S-23, phase-I metabolism followed by sulfonation.

ence to **M3** was determined using the above described high resolution/high accuracy LC-MS setup.

Results and Discussion

In vitro metabolism studies

All *in vitro* metabolism studies were conducted using established assays employing the co-substrates NADPH, UDPGA or PAPS, and enzymatic fractions of human liver (microsomes and S-9). Since only marginal differences in phase-I metabolism were observed between HLM and S-9 fractions (data not shown), all results discussed in the following were obtained from incubation reactions with the S-9 fraction only. The metabolic reactions were carried out in two different sets allowing either glucuronidation or sulfonation as phase-II-reactions, and generated metabolites were characterized by low- and high-resolution (tandem) mass spectrometry by means of accurate masses of precursor and product ions as well as typical collision-induced dissociation (CID) pathways. Due to the lack of reference material for most metabolic products, absolute quantitation of the analytes in incubation mixtures was not possible; hence, relative abundances were calculated from low resolution full scan mass spectrometric analyses by extracting respective ion traces of deprotonated molecules and integration of peak areas. These values were used

for a rough estimation of each metabolite's contribution to the sum of the measured metabolic products as illustrated in Figure 3.

The incubation of S-22 with co-substrates enabling phase-I-reactions followed by glucuronidation predominantly yielded the glucuronic acid conjugates of the active drug S-22 (Figure 2; **M4**, 49%) as well as the mono- and bishydroxylated analogs (**M5**, 19%, and **M6**, 7.5%, respectively) as illustrated in Figure 3A. The major unconjugated metabolites detected in the reaction mixture were **M3** (O-dephenylation, 18%) and **M1** (monohydroxylation, 6%), and minor amounts of the bishydroxylated product (**M2**, 0.5%) were observed. In contrast to the efficient glucuronidation reactions, a rather limited conjugation to sulfates was found. Only 1% of the monohydroxylated and 4% of the bishydroxylated S-22 was found sulfonated (**M7** and **M8**, respectively, Figure 3B) while the majority of phase-I-metabolites (**M1–M3**) remained unchanged during *in vitro* incubations. Moreover, no sulfate of the intact S-22 was detected after *in vitro* incubation with human liver fractions.

The *in vitro* metabolism of S-23 yielded, qualitatively, nearly identical results as found with S-22. Except for **M8** (bishydroxylation and sulfonation), all metabolic products corresponding to **M1–M7** of S-22 were detected. Quantitatively, considerable differences were observed as S-23 was predominantly monohydroxylated and glucuronidated (**M5**, 55%) in respective *in vitro* experiments (Figure 3C). Glucuronidation of S-23 (**M4**) and bishydroxylation followed by glucuronic acid conjugation (**M6**) accounted for 5%

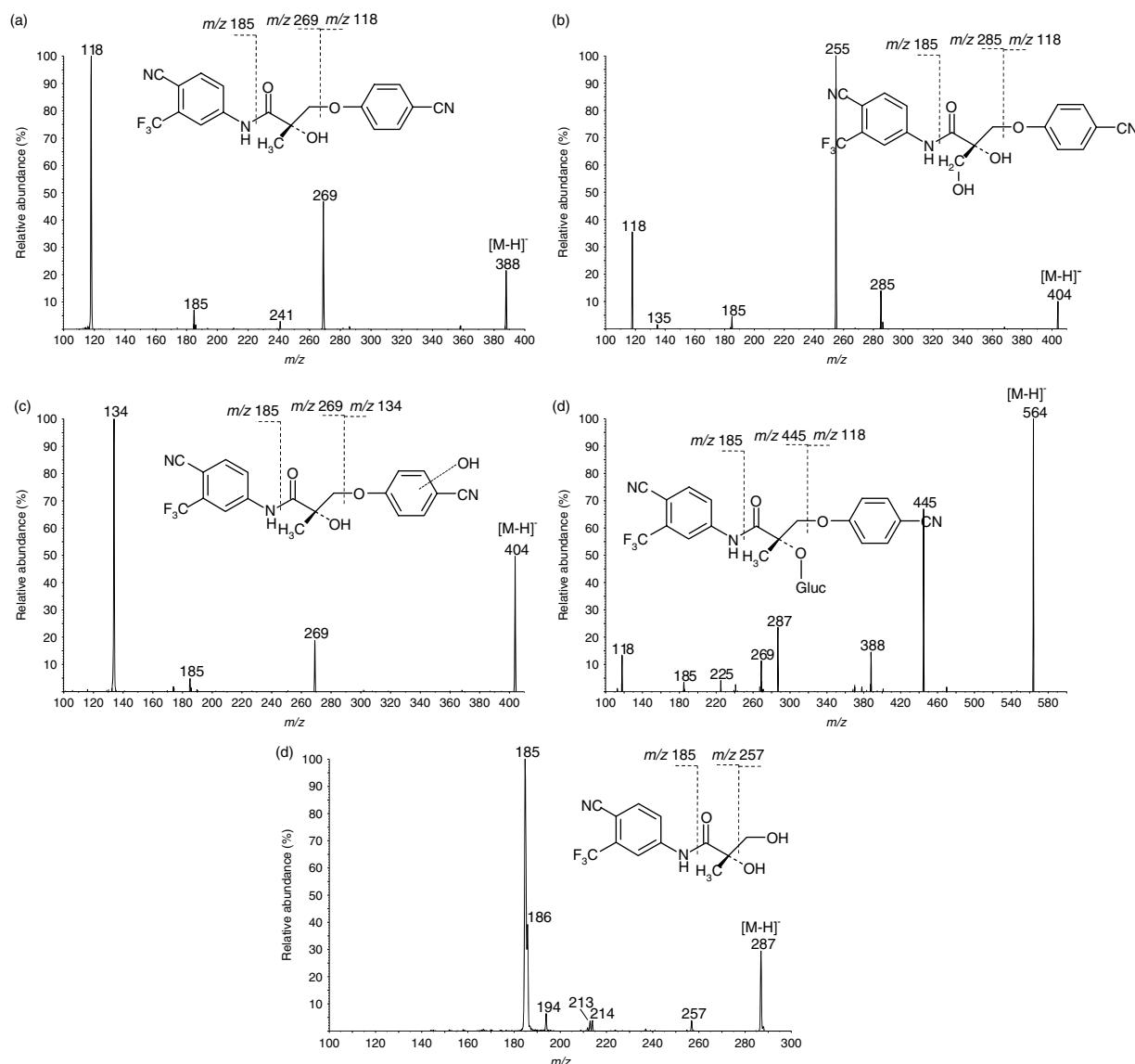


Figure 4. ESI product ion spectra of $[M - H]^-$ ions of a) S-22, b) **M1a**, c) **M1c**, d) **M4**, and e) **M3**.

and 4%, respectively, and unconjugated metabolites in consecutive phase-I/phase-II (glucuronidation) metabolism experiments were represented mainly by **M1** (6%) and **M3** (30%). The share of **M2** (bishydroxylated S-23) was less than 0.5% and was not further considered. In case of combined phase-I and phase-II sulfonation metabolism reactions, a distribution of metabolites comparable to S-22 was observed (Figure 3D) with **M1** (monohydroxylated S-23) being the most abundant product accounting for 57% of the generated compounds. Further, bishydroxylation (**M2**, 33%), dephenylation (**M3**, 6%) as well as monohydroxylation and sulfonation (**M7**, 4%) were detected while **M8** (the sulfonated **M2**) was not observed.

The structures and compositions of metabolites were deduced from accurately measured molecular masses and characteristic dissociation routes of deprotonated molecules under CID conditions (Tables 1 and 2). In Figure 4, the product ion mass spectra of S-22 (a), its monohydroxylated metabolites **M1a** (b) and **M1c** (c), as well as the glucuronic acid conjugate of S-22 (**M4**, d) are depicted as typical examples for mass spectrometry-derived infor-

mation allowing structure elucidation of target compounds. The active drug S-22 dissociates upon collisional activation yielding abundant product ions at m/z 269, 241, 185, and 118. The latter represents the intact B-ring structure as the 4-cyanophenol anion and m/z 185 the intact A-ring as the deprotonated 4-cyano-3-trifluoromethyl aniline, while m/z 269 is the counterpart to m/z 118 with an assumed epoxide structure.^[9] The subsequent loss of carbon monoxide (-28 Da) from m/z 269 further leads to m/z 241.

Hydroxylation and/or conjugation of either parts of S-22 cause diagnostic shifts of these product ions that allow the approximate or precise localization of modifications. The hydroxylation of **M1a** was suggested to reside at the methyl group attached to the chiral carbon atom due to the presence of m/z 118 and 185 (representing the unmodified B- and A-rings, respectively) and the absence of m/z 269, which was incremented by 16 Da to m/z 285. The hydroxylation was consequently assigned to the core moiety of S-22, and the elimination of formaldehyde (-30 Da) from m/z 285 yielding the base peak at m/z 255 (Figure 4B) provided evidence for the presence of a hydroxymethyl function in the

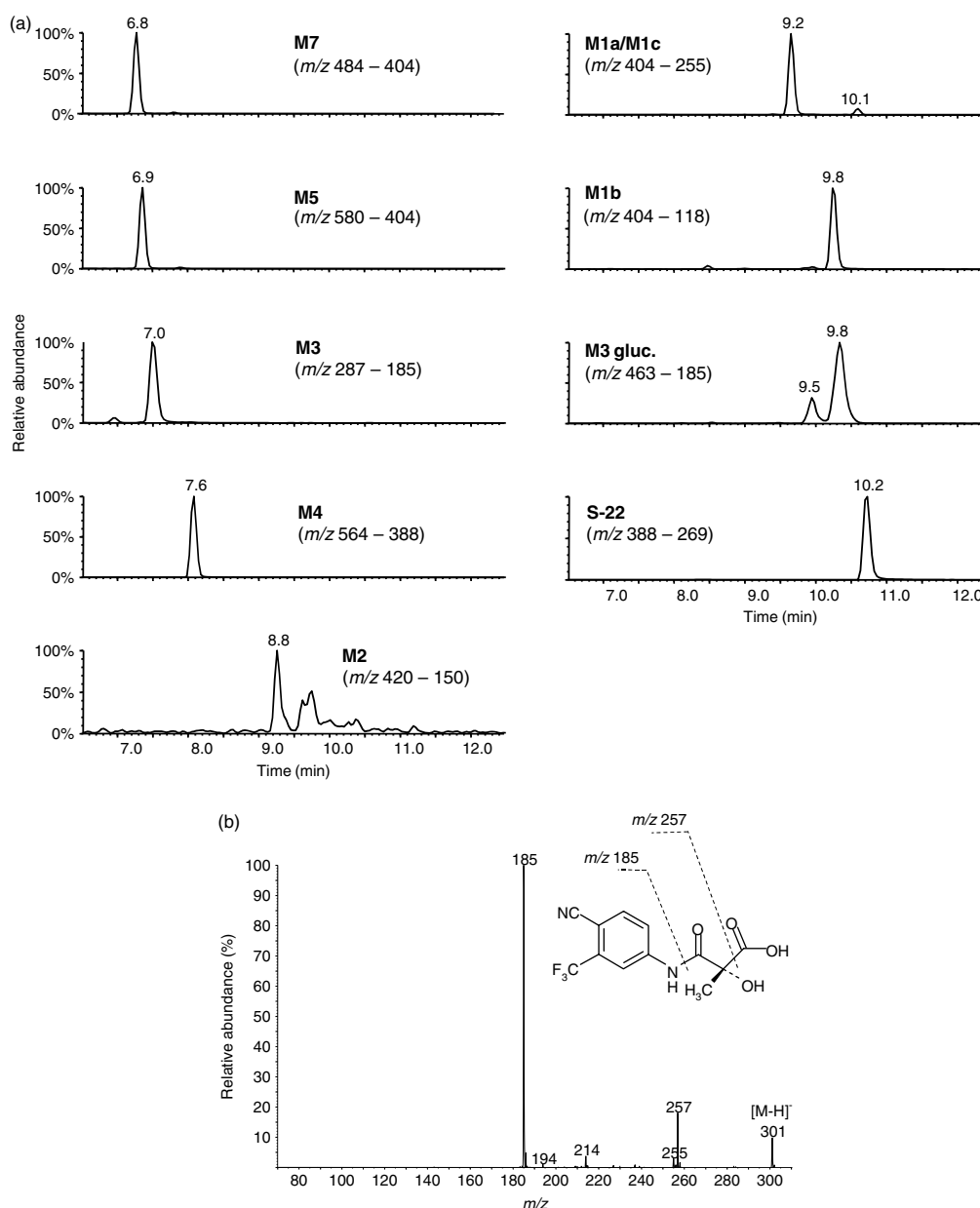


Figure 5. (A) Compiled extracted ion chromatograms of metabolites found between 24 and 48 h after oral high-dose application of S-22 as measured using diagnostic ion transitions for respective analytes. The same metabolic pattern was observed in all three urine pools with **M3** and **M4** being the most abundant analytes in all samples. (B) Product ion mass spectrum of $[M-H]^-$ of **M3-c** found only in canine urine, representing approximately 30% of the observed metabolic products of S-22.

intact molecule. In contrast, the product ion mass spectrum of the deprotonated molecule of **M1c** contained the characteristic ions of an intact A-ring and arylpropionamide core structure (i.e. m/z 185 and 269, respectively) but the B-ring was found hydroxylated as demonstrated by the ion at m/z 134 resulting from m/z 118 and the addition of oxygen (Figure 4C). The question whether the hydroxyl group is located in ortho- or meta-position remained to be clarified. The glucuronidation site of S-22 was assumed to be the hydroxyl function at the chiral carbon atom and product ions derived from **M4** under CID conditions confirmed the conjugation site (Figure 4D). The ion at m/z 269 was detected but also its counterpart incremented by 176 Da to yield m/z 445 while m/z 118 and 185 did not produce analogous fragments shifted by the typical mass of a glucuronic acid moiety. Furthermore, the

deprotonated aglycon was found at m/z 388 (Figure 4A). An interesting observation was made with m/z 287 in the product ion mass spectrum of **M4**, which was found to be a water adduct of m/z 269, generated only from **M4** under MS/MS conditions. The fact that ion-molecule reactions occur in ion traps has been reported manifold, and water molecules have shown to be frequent reaction partners.^[29–32]

The mass spectral behaviour of S-23 and its metabolites was in agreement with the dissociation routes observed with S-22, and metabolic products were assigned accordingly (Table 2). A common metabolite of both drug candidates was identified and referred to as **M3**, the dephenylated (or B-ring depleted) molecule of S-22 and S-23 (Figure 2). Due to its great potential to serve as a target analyte for doping control purposes covering more than

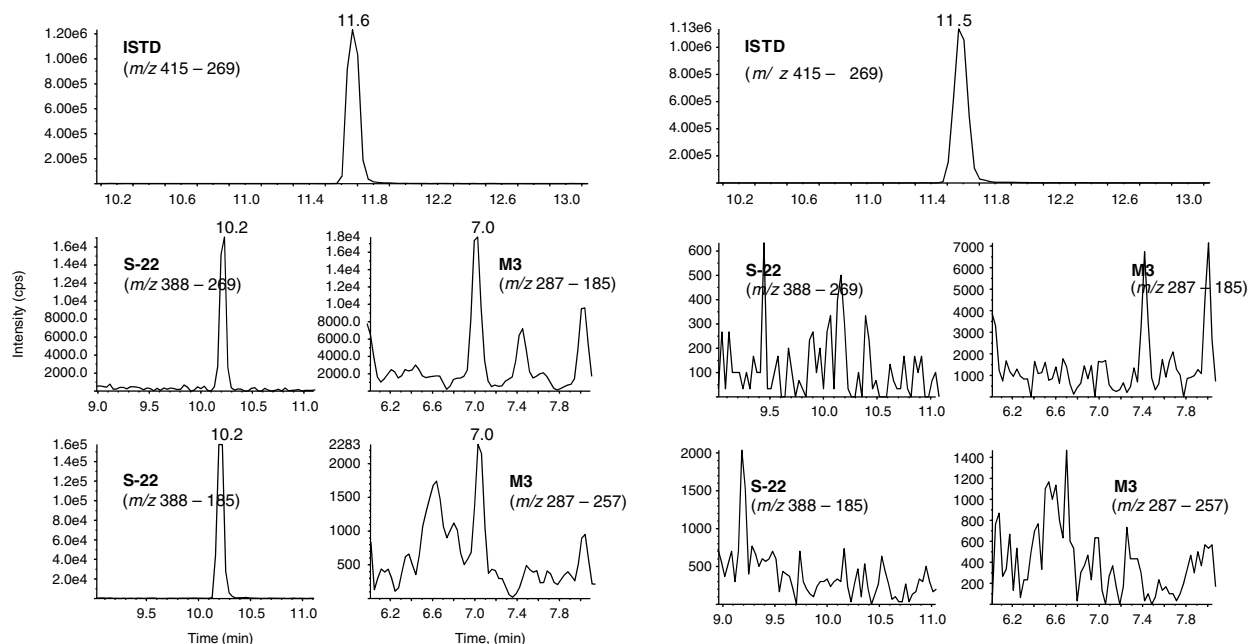


Figure 6. Extracted ion chromatograms of the analysis of a 48–72 h urine pool following low-dose administration of S-22 (left) and a blank urine specimen (right). The intact drug (S-22) in particular as well as **M3** are still clearly visible.

only one banned substance, **M3** was synthesized and characterized by NMR and high resolution/high accuracy mass spectrometry. ^1H NMR (CDCl_3) δ (ppm): 1.47 (s, 3H, H-21), 3.33 (s, 1H), 3.60 (dd, 1H, H-3a, $J = 10.8/3.8$ Hz), 4.16 (dd, 1H, H-3b, $J = 10.8/3.8$ Hz), 7.80 (d, 1H, H-15, $J = 8.5$ Hz), 7.93 (dd, 1H, H-14, $J = 8.5/2.1$ Hz), 8.10 (d, 1H, H-18, $J = 2.1$ Hz), 9.01 (s, 1H). ^{13}C NMR (HMQC/HMBC) δ (ppm): 22.5 (C-21), 67.5 (C-3), 76.7 (C-2), 104.9 (C-16), 115.6 (C-13), 117.2 (C-18), 121.7 (C-14), 134.2 (C-20/19), 135.9 (C-15), 141.5 (C-17), 173.7 (C-1). The product ion mass spectrum of **M3** is illustrated in Figure 4E yielding mainly one abundant product ion at m/z 185, which was attributed to the above reported A-ring fragment of other metabolites. In addition, the loss of $\text{C}_3\text{H}_6\text{O}_2$ (–74 Da) representing the 1,2-bishydroxypropanol residue under migration of one hydrogen to the charge-retaining part of the molecule [N-(4-cyano-3-trifluoromethyl-phenyl)-formamide] was suggested to yield the low-abundant ion at m/z 213. The elimination of formaldehyde (–30 Da) from the deprotonated molecule of **M3** gave rise to m/z 257.

Implementation of potential metabolites in doping control procedure

After characterization of the *in vitro* generated metabolites, the potential target analytes were implemented into an existing doping control screening procedure using two or three ion transitions per compound (Tables 1 and 2). Specificity was tested for each substance, and no interference was observed at respective retention times. Ion suppression/enhancement effects were less than 10% for all analytes' retention times.

Administration study dog urine samples

In order to obtain proof-of-concept, canine urine samples were collected after oral administration of S-22 at two different dosages (low: 0.0314 mg/kg and high: 30 mg/kg) and analyzed using the above reported initial testing procedure. Specimens

were obtained prior to application of S-22 and as 24 h-pools covering the periods 0–24 h, 24–48 h, and 48–72 h. Except for **M6** and **M8**, all metabolites generated using the *in vitro* assay were found in the administration studies (Table 1), and a compilation of extracted ion chromatograms of the 24–48 h specimen of the high-dose study is illustrated in Figure 5A. Noteworthy, the glucuronic acid conjugate of **M3** was detected in canine post-administration samples (Figure 5A, 9.5/9.8 min) but not using the *in vitro* metabolism approach, and the most prominent urinary metabolite generated *in vivo* was suggested to represent the carboxyl analog to **M3** (**M3-c**, Figure 5B), which was also not formed by incubating S-22 in human liver microsomal preparations. The elemental composition of **M3-c** was determined by high resolution/high accuracy mass spectrometry revealing $\text{C}_{12}\text{H}_8\text{O}_4\text{N}_2\text{F}_3$ (error: –1.3 ppm), and further evidence for the proposed structure was obtained by typical collision-induced dissociation pathways indicating the presence of a carboxyl function. These include the elimination of carbon dioxide (–42 Da) and formic acid (–44 Da) to generate the product ions at m/z 257.0541 (error: –1.1 ppm) and 255.0384 (error: –1.1 ppm), respectively (not shown). The intact A-ring was evidenced by the presence of m/z 185.0328 (error: –2.4 ppm).

Concerning the traceability of an S-22 administration, the metabolites **M3** and **M4** proved particularly useful as they were detected in the 48–72 h urine pool of the low-dose excretion study (Figure 6) and therefore represent potential target analytes for future doping control purposes. One of the primary goals of sports drug testing is to provide extended detection windows for prohibited compounds, especially for drugs that exhibit beneficial effects even weeks after cessation. Consequently, those metabolites being detectable for the longest period are considered optimal analytes for efficient sports drug testing programmes. It must be noted, however, that the above-reported data were obtained from animal models and can serve only as proof-of-concept as species-specific metabolism and excretion might reveal deviating elimination pathways and profiles in humans.

Conclusion

The misuse of emerging drugs for performance enhancement has been known to be a considerable threat to the integrity of sport. Due to the fact that such compounds are occasionally available even years before clinical trials are finalized, sports drug testing authorities need to test for these agents ahead of the pharmaceutical launch to minimize the 'window of opportunity' provided to cheating athletes. In order to enable the detection of drug administration by means of urine specimens, metabolism studies are required such as those conducted for two emerging SARM candidates in the present study. In general, *in vitro* simulation of metabolic reactions has shown a considerable correlation to *in vivo* obtained metabolites, thus outlining its utility as a rapid and cost-effective tool to provide first insights into the metabolic conversion of new therapeutics. As an alternative to the herein discussed approach, recently reported animal models with humanized liver could also be utilized as described for anabolic androgenic steroids.^[33,34] These might, however, require more technical and financial resources in order to enable the animal preparation and adequate welfare. Moreover, the use of intact human liver cells was successfully employed for the metabolism of designer steroids,^[35] showing another option to prepare and identify target analytes and common metabolic routes of drugs. These efforts will support the sensitive and specific determination of emerging therapeutics in doping controls, which can further be compared to future administration studies.

Acknowledgments

The study was carried out with support of the World Anti-Doping Agency and the Federal Ministry of the Interior of the Federal Republic of Germany. The authors further gratefully acknowledge support of the presented work by GTx, Inc., (Memphis, TN, USA).

References

- [1] M. L. Mohler, C. E. Bohl, R. Narayanan, Y. He, D. J. Hwang, J. T. Dalton, D. D. Miller, in *Nuclear Receptors as Drug Targets*, (Eds: E. Ottow, and H. Weinmann), Wiley-VCH: Weinheim, **2008**, pp. 249.
- [2] M. L. Mohler, C. E. Bohl, A. Jones, C. C. Coss, R. Narayanan, Y. He, D. J. Hwang, J. T. Dalton, D. D. Miller, *J. Med. Chem.* **2009**, *52*, 3597.
- [3] S. Bhasin, R. Jasuja, *Curr. Opin. Clin. Nutr. Metab. Care.* **2009**, *12*, 232.
- [4] W. Gao, J. T. Dalton, *Drug Discov. Today* **2007**, *12*, 241.
- [5] E. J. Kilbourne, W. J. Moore, L. P. Freedman, S. Nagpal, *Curr. Opin. Investig. Drugs* **2007**, *8*, 821.
- [6] W. Gao, J. Kim, J. T. Dalton, *Pharm. Res.* **2006**, *23*, 1641.
- [7] M. Thevis, H. Geyer, M. Kamber, W. Schänzer, *Drug Test. Anal.* **2009**, *1*, 387.
- [8] World Anti-Doping Agency, **2010**, Available at: http://www.wada-ama.org/Documents/World_Anti-Doping_Program/WADP-Prohibited-list/WADA_Prohibited_List_2010_EN.pdf [14 January 2010].
- [9] M. Thevis, M. Kamber, W. Schänzer, *Rapid Commun. Mass Spectrom.* **2006**, *20*, 870.
- [10] M. Thevis, M. Kohler, J. Maurer, N. Schlörner, M. Kamber, W. Schänzer, *Rapid Commun. Mass Spectrom.* **2007**, *21*, 3477.
- [11] M. Thevis, M. Kohler, N. Schlörner, G. Fusshöller, W. Schänzer, *Eur. J. Mass Spectrom.* **2008**, *14*, 153.
- [12] M. Thevis, M. Kohler, A. Thomas, N. Schlörner, W. Schänzer, *Rapid Commun. Mass Sp.* **2008**, *22*, 2471.
- [13] M. Thevis, W. Lohmann, Y. Schrader, M. Kohler, W. Bornatsch, U. Karst, W. Schänzer, *Eur. J. Mass Spectrom.* **2008**, *14*, 163.
- [14] M. Thevis, W. Schänzer, *J. Mass Spectrom.* **2008**, *43*, 865.
- [15] C. E. Bohl, C. Chang, M. L. Mohler, J. Chen, D. D. Miller, P. W. Swaan, J. T. Dalton, *J. Med. Chem.* **2004**, *47*, 3765.
- [16] J. Kim, D. Wu, D. J. Hwang, D. D. Miller, J. T. Dalton, *J. Pharmacol. Exp. Ther.* **2005**, *315*, 230.
- [17] D. Yin, H. Xu, Y. He, L. I. Kirkovsky, D. D. Miller, J. T. Dalton, *J. Pharmacol. Exp. Ther.* **2003**, *304*, 1323.
- [18] R. Narayanan, C. C. Coss, M. Yepuru, J. D. Kearbey, D. D. Miller, J. T. Dalton, *Mol. Endocrinol.* **2008**, *22*, 2448.
- [19] J. Chen, D. J. Hwang, C. E. Bohl, D. D. Miller, J. T. Dalton, *J. Pharmacol. Exp. Ther.* **2005**, *312*, 546.
- [20] A. Jones, J. Chen, D. J. Hwang, D. D. Miller, J. T. Dalton, *Endocrinology* **2009**, *150*, 385.
- [21] T. Kuuranne, A. Leinonen, W. Schänzer, M. Kamber, R. Kostianen, M. Thevis, *Drug Metab. Dispos.* **2008**, *36*, 571.
- [22] W. Gao, Z. Wu, C. E. Bohl, J. Yang, D. D. Miller, J. T. Dalton, *Drug Metab. Dispos.* **2006**, *34*, 243.
- [23] M. A. Perera, D. Yin, D. Wu, K. K. Chan, D. D. Miller, J. Dalton, *Drug Metab. Dispos.* **2006**, *34*, 1713.
- [24] R. Dams, M. A. Huestis, W. E. Lambert, C. M. Murphy, *J. Am. Soc. Mass Spectrom.* **2003**, *14*, 1290.
- [25] B. K. Matuszewski, M. L. Constanzer, C. M. Chavez-Eng, *Anal. Chem.* **2003**, *75*, 3019.
- [26] C. A. Marhefka, W. Gao, K. Chung, J. Kim, Y. He, D. Yin, C. Bohl, J. T. Dalton, D. D. Miller, *J. Med. Chem.* **2004**, *47*, 993.
- [27] H. Tucker, G. J. Chesterson, *J. Med. Chem.* **1988**, *31*, 885.
- [28] H. Tucker, J. W. Crook, G. J. Chesterson, *J. Med. Chem.* **1988**, *31*, 954.
- [29] A. B. Attygalle, N. Kharbatia, J. Bialecki, J. Ruzicka, A. Svatos, E. J. Stauber, *Rapid Commun. Mass Spectrom.* **2006**, *20*, 2265.
- [30] L. A. Moraes, M. N. Eberlin, *J. Mass Spectrom.* **2002**, *37*, 162.
- [31] A. Weisz, D. Andrzejewski, H. M. Fales, A. Mandelbaum, *J. Mass Spectrom.* **2002**, *37*, 1025.
- [32] S. Beuck, T. Schwabe, S. Grimme, N. Schlörner, M. Kamber, W. Schänzer, M. Thevis, *J. Am. Soc. Mass Spectrom.* **2009**, *20*, 2034.
- [33] L. Lootens, P. Meuleman, O. J. Pozo, P. Van Eenoo, G. Leroux-Roels, F. T. Delbeke, *Clin. Chem.* **2009**, *55*, 1783.
- [34] O. J. Pozo, L. Lootens, P. Van Eenoo, K. Deventer, P. Meuleman, G. Leroux-Roels, M. K. Parr, W. Schänzer, F. T. Delbeke, *Drug Test. Anal.* **2009**, *1*, 554.
- [35] J. F. Levesque, E. Templeton, L. Trimble, C. Berthelette, N. Chauret, *Anal. Chem.* **2005**, *77*, 3164.